第 31 卷第 11 期
2015 年 11 月

无 机 化 学 学 报
CHINESE JOURNAL OF INORGANIC CHEMISTRY

Vol.31 No.11
2103-2110

由酰胺四酸配体构建的一个微孔三维金属有机骨架化合物及其高效可逆碘吸附性能

杭 成 卢治拥 孟 飞 江静静 白俊峰*
(南京大学化学化工学院配位化学国家重点实验室,南京 210093)

摘要: 合成并表征了一个由酰胺键修饰并带有 π-电子内壁的微孔三维金属有机骨架化合物[$Cu_5(L)_2(H_2O)_5$] (**1**) (H_4L=5,5′-((1*H*-pyrazole-3,5-dicarbonyl)bis(azanediyl))diisophthalic))。拓扑分析表明 **1** 为(3,3,4,4,6)-连接类型的网络结构,同时通过氮气和二氧化碳气体吸附验证了其孔道性质。同时 **1** 可以作为碘分子吸附的良好主体(1.94 mmol·g^{-1},室温),并在碘分子的可逆吸附中具有出色的表现。

关键词: 金属有机骨架化合物; 酰胺键; π-电子; 碘吸附
中图分类号: O614.121 **文献标识码**: A **文章编号**: 1001-4861(2015)11-2103-08
DOI: 10.11862/CJIC.2015.276

A Microporous 3D MOF Constructed from an Acylamide Tetracid Ligand: Effective Reversible Iodine Adsorption Property

HANG Cheng LU Zhi-Yong MENG Fei JIANG Jing-Jing BAI Jun-Feng*
(*State Key Laboratory of Coordination Chemistry, School of Chemistry and Chemical Engineering, Nanjing University, Nanjing* 210093, *China*)

Abstract: A microporous 3D MOF, [$Cu_5(L)_2(H_2O)_5$] (**1**) (H_4L=5,5′-((1*H*-pyrazole-3,5-dicarbonyl)bis(azanediyl)) diisophthalic)) with acylamide-functionalized and π-electron walls in its structure was synthesized and characterized. Topological analysis reveals **1** is of 3,3,4,4,6-c net and its porosity was tested by N_2 and CO_2 gas adsorption. Meanwhile, **1** can serve as a good host for encapsulating I_2 (1.94 mmol·g^{-1}, RT) and exhibits an outstanding performance in reversible adsorption of iodine molecules. CCDC: 1417058.

Key words: metal-organic frameworks (MOFs); acylamide bond; π-electron; adsorption of iodine

0 Introduction

Metal-organic frameworks (MOFs), which belong to a class of well-ordered porous crystalline materials, have attracted continuous interest due to their controllable structures and various potential applications in gas storage or separation, catalysis, chemical sensing, luminescence and so on[1]. In contrast to these traditional and seemingly bottlenecked study of MOFs, the research based on the specific host-guest interactions in capsulation of functional species such as drugs, dyes, and light emitters into cavities of MOFs is an arising and promising study point. As we know, a superiority of MOF materials is that we can realize more specialized applications by introducing specific functional groups into the frameworks. With these

收稿日期:2015-07-30。收修改稿日期:2015-09-09。
国家自然科学基金(No.21371091, 21371150)资助项目。
*通讯联系人。E-mail:bjunfeng@nju.edu.cn

functional groups, we can modify the physical environment of pores and surfaces in the frameworks and thus tune the interactions between frameworks and guest species.

Iodine, since discovered in 1811 by French chemist Courtois[2] and its application in life science[3], marine atmosphere[4], material science[5], especially its role in the 2011 disaster at Japan′s Fukushima Dai-Ichi nuclear energy centre, has attracted growing attention and more research enthusiasm from scientists. As a natural-scarce resource and very important element, iodine is of great demand in many fields and its effective capture and storage has been a valuable study focus. In some works reported recently, some microporous and amide-modified MOFs were used as the fine hosts in rapid and reversible adsorption of iodine[6-7]. From these works, we can deduce that by introducing acylamide and aromatic groups into the frameworks and thus through the host-guest π-bonding and hydrogen-bonding formed between these groups and the iodine molecules, we may enhance the adsorbent-adsorbate interactions to sharply improve iodine adsorption in MOFs. Herein, we report a novel microporous 3D Cu-MOF ($[Cu_5(L)_2(H_2O)_5]$ (**1**), (H_4L=5,5′-((1*H*-pyrazole-3,5-dicarbonyl)bis(azanediyl)) diisophthalic)) (Fig.1a) in which there are square-like channels (dimension *ca.* 0.67 nm×0.67 nm) surrounded with aromatic rings (benzene and pyrazole rings) and acylamide groups which create a suitable environment abundant with adsorption binding sites for I_2.

1 Experimental

1.1 Material and measurements

All chemical reagents were obtained from commercial sources and, unless otherwise noted, were used as received without further purification. Elemental analysis (C, H, and N) was performed on a Perkin-Elmer 240 analyzer. The IR spectra were recorded in the 400~4 000 cm^{-1} on a VECTOR TM 22 spectrometer using KBr pellets. ^1H NMR spectra were recorded on a Bruker DRX-500 spectrometer with tetramethylsilane as an internal reference. Powder X-ray diffraction (PXRD) data was collected on a Bruker D8 ADVANCE X-ray diffractometer with Cu Kα radiation.

1.2 Synthesis of H_4L

A mixture of 1*H*-pyrazole-3,5-dicarboxylic acid (2 g, 11.49 mmol), freshly distilled thionyl chloride (80 mL, 1.1 mol), and a few drops of DMF was heated to reflux for 12 h. Excess thionyl chloride was removed by distillation under reduced pressure and the resulting white powder was used as such. To this was added 5-aminoisophthalic acid (4.37 g, 24.13 mmol), DMA (50 mL), and *N*,*N*-dimethyl-4-aminopyridine (0.25 g, 2 mmol), after which the solution was stirred in ice bath for 12 h. The resultant mixture was poured into water, and the precipitate that formed was filtered off, extracted with hot methanol several times and dried in vacuum at 70 ℃ (Scheme 1). Yield: 70%. Selected IR (KBr, cm^{-1}): ^1H NMR (500 MHz, DMSO-d_6) δ: 14.50(s, 1H), 13.28(s, 4H), 10.72(s, 2H), 8.69(s, 4H), 8.23(s, 2H), 7.75(s, 1H). IR (cm^{-1}, KBr): 3 316, 3 144, 1 737, 1 568, 1 400, 1 214, 757.

1.3 Preparation of 1

A mixture of $Cu(NO_3)_2\cdot 6H_2O$ (11.6 mg, 0.048 mmol), H_4L (5.8 mg, 0.012 mmol), HNO_3 (160 μL, 16 mol·L^{-1}), *N*,*N*-dimethylformamide (DMF) (1.65 mL)/deionized water(0.35 mL) was stirred for ca. 20 min in air then transferred and sealed in a 20 mL Pyrex tube, which was then heated at 85 ℃ for 48 h. The obtained blue bulk crystals of **1** were filtered and washed with DMF. Yield: 60% (based on H_4L). Anal. Calcd. for evacuated samples of **1** ($C_{42}H_{28}Cu_5N_8O_{20}$, %): C, 39.34; H, 2.20; N, 8.74; Found (%): C, 39.30; H, 2.40; N, 8.78. IR (KBr, cm^{-1}): 3 395, 2 361, 1 561, 1 364, 769, 720, 677.

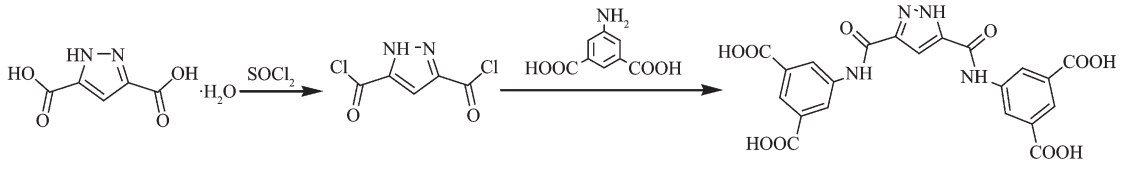

Scheme 1 Schematic view of the synthesis of H_4L

1.4 Single crystal X-ray diffraction analysis

The crystal of **1** was sealed in a capillary under a microscope with some mother liquor inside to prevent desolvation and the single X-ray diffraction data was measured on a Bruker smart Apex Ⅱ CCD diffractometer at 293 K using graphite monochromated Mo $K\alpha$ radiation (λ=0.071 073 nm). Data reduction was made with the Bruker Saint program. The structure was solved by direct methods and refined with full-matrix least squares technique using the SHELXTL package[8]. Non-hydrogen atoms were refined with anisotropic displacement parameters during the final cycles. Hydrogen atoms of the ligands were placed in calculated positions with isotropic displacement parameters set to $1.2U_{eq}$ of the attached atoms. In the crystal, free solvent molecules were highly disordered, and it was unsuccessful to attempt to locate and refine the solvent peaks. The diffused electron densities resulting from these residual solvent molecules were removed from the data set using the SQUEEZE routine of PLATON[9] and further refined using the data generated. The contents of the solvent region are not represented in the unit cell contents in the crystal data and the hydrogen atoms of the water molecules were not included in the model. Crystal data and further information on the structure determination are summarized in Table 1.

CCDC: 1417058.

Table 1　Crystal data and structural refinement summary for complex 1

Formula	$C_{42}H_{18}Cu_5N_8O_{25}$	Crystal size / mm	0.27×0.25×0.22
Formula weight	1 352.4	θ range for data collection / (°)	0.74~25.0
Crystal system	Orthorhombic	Reflections collected unique	18 964
Space group	*Pbcm*	Completeness / %	100
a / nm	2.767 0(6)	Absorption correction	Semi-empirical from equivalents
b / nm	2.929 7(6)	Max. and min. transmission	0.795 and 0.762
c / nm	2.591 2(6)	Data /restraints / parameters	18 964 / 96 / 652
Volume / nm^3	21.006(8)	Goodness-of-fit on F^2	1.068
Z	8	Final R^a indices [$I>2\sigma(I)$]	R_1=0.091 0, wR_2=0.190 5
D_c / ($g\cdot cm^{-3}$)	0.855	R^a indices (all data)	R_1=0.127 7, wR_2=0.207 5
Absorption coefficient / mm^{-1}	1.042	Largest diff. peak and hole / ($e\cdot nm^{-3}$)	1 515 and −776
F(000)	5 368		

$^aR_1=\sum||F_o|-|F_c||/|F_o|$; $wR_2=[\sum w(\sum F_o^2-F_c^2)^2/\sum w(F_o^2)^2]^{1/2}$

1.5 Gas adsorption experiments

In the gas sorption measurements, all the gases used are of 99.999% purity. Low-pressure N_2 (77 K) and CO_2 (273 K, 298 K) adsorption measurements (up to 101 kPa) were performed on Micromeritics ASAP 2020 M surface area analyzer.

1.6 Iodine sorption experiments

The as-synthesized samples of **1** (40 mg) after washed and soaked with DMF for days were immersed in a hexane (3 mL) solution of I_2 (0.01 $mol\cdot L^{-1}$), to give I_2@**1**. The photographs of the crystals were used to determine the adsorption ability. The crystals of I_2@**1** (10 mg) were soaked in anhydrous ethanol (5 mL), and UV-Vis spectra and photographs were used to determine the desorption ability.

2 Results and discussion

2.1 Crystal structure description

In the asymmetric unit of **1**, there are five Cu^{2+} ions, two deprotoned H_4L ligands, and five coordinated water molecules (Fig.1b). Two kinds of Cu clusters exist in the whole structure: one is the Cu paddle-wheel in which two water molecules occupy the axial position and four deprotoned carboxylate groups from different ligands take up the equatorial position; the other one is pyrazole-bridged cyclic binuclear complex in which the dihedral angle between the two pyrazole rings is 113.25° and the five-coordinated Cu1 is in pyramidal configuration with N1, N3, O8, O9 in the flat position and O1 in the vertical position, while the

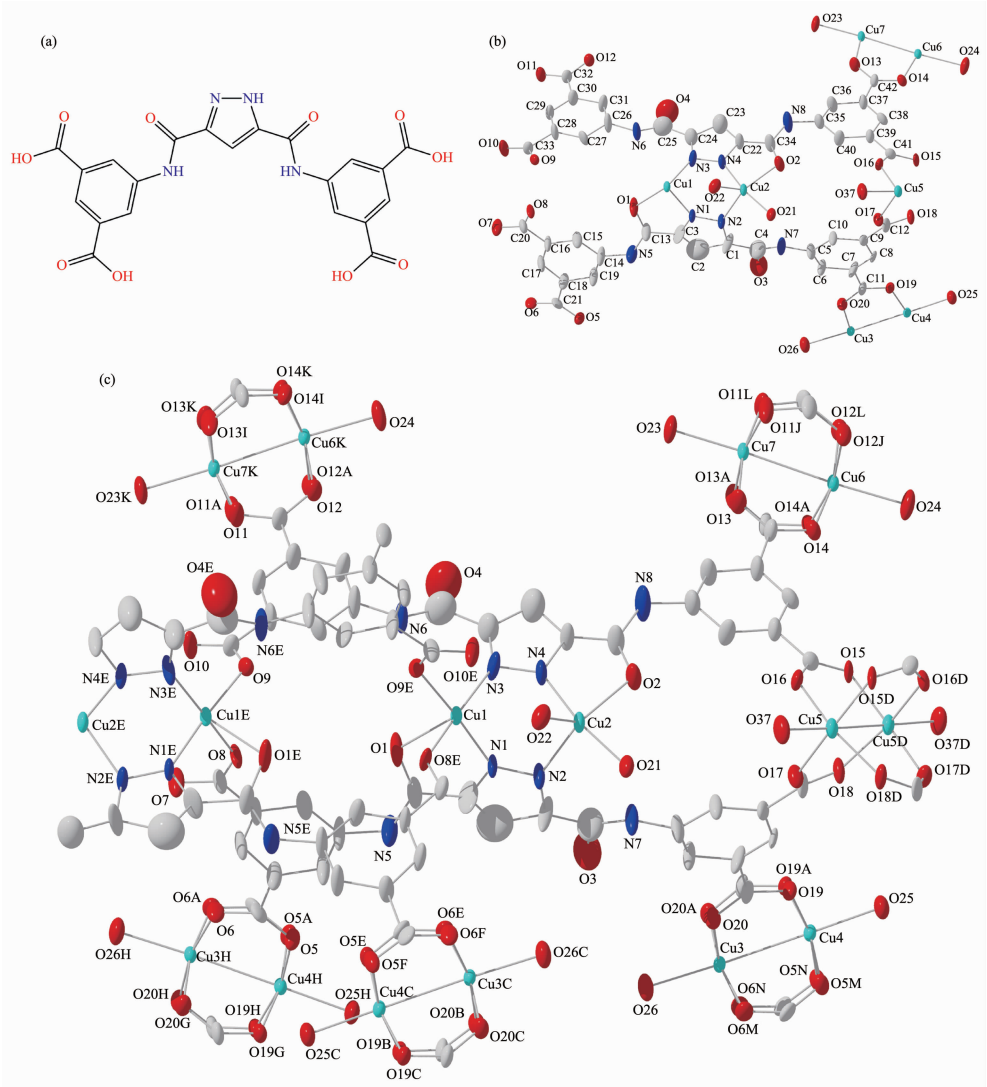

Symmetry codes in (c): A: x, y, 0.5−z; B: −x, 1−y, −z; C: −x, 1−y, −0.5+z; D: x, 1.5−y, −z; E: x, 0.5−y, −z; F: x, 0.5−y, −0.5+z; G: −x, −0.5+y, z; H: −x, −0.5+y, 0.5−z; I: 1−x, −0.5+y, z; J: 1−x, 0.5+y, z; K: 1−x, −0.5+y, 0.5−z; L: 1−x, 0.5+y, 0.5−z; M: −x, 0.5+y, z; N: −x, 0.5+y, 0.5−z

Fig.1 (a) Structure of the carboxylate ligand (H_4L) used in this paper; (b) View of asymmetric unit of **1** with thermal ellipsoids shown at 30% probability; (c) View of the coordination environment of the Cu clusters in the structure with thermal ellipsoids shown at 30% probability

five-coordinated Cu2 is in distorted trigonal bipyramidal configuration with N2, O2, O22 in the flat position and N4, O21 in the vertical position (Fig.1c). Topological analysis was carried out with the TOPOS software[10]: The Cu paddlewheel units are simplified as four-connected nodes and the binuclear copper clusters with two bidentate pyrazole-3,5-diacylamide parts, two water molecules coordinated to Cu2, and two carboxyl groups coordinated to Cu1 are simplified as six-connected nodes, and the benzene rings as three-connected nodes. Consequently, the whole structure of **1** can be described as a 5-nodal (3,3,4,4,6)-c net with the stoichiometry $(3\text{-c})_4(3\text{-c})_4(4\text{-c})_2(4\text{-c})(6\text{-c})_2$. Surprisingly, while the spatial arrangements of these SBUs (Secondary Building Units) seemed disordered, in the whole structure there exist parallel square nano-tubular channels (0.67 nm×0.67 nm) (Fig. 2a) along b axis in which nearly all the aromatic rings and acylamide groups of ligands are paved levelly in the surface which are thus filled with potential adsorption binding sites for iodine molecules with proper size (the van der Waals diameter of I_2

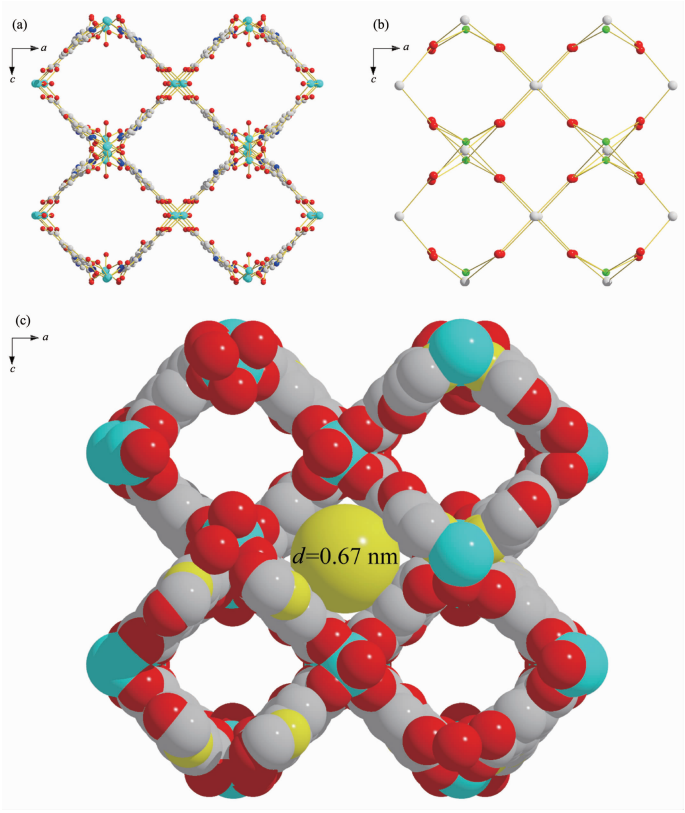

Fig.2　(a) One-dimensional cubic nano-tubular channels (0.67 nm×0.67 nm) along the *b* axis; Channels are occupied with disordered DMF solvent molecules and water molecules in the as-synthesized crystals; Total accessible volume (13.604 2 nm^3) is 64.8% per unit cell (21.006 nm^3) as calculated by PLATON[9]; (b) Topologic network of **1**; (c) Space-filling mode of **1** and the pore size of the channels along the *b* axis are estimated by the ball in the channels

molecules is 0.396 nm).

2.2　Thermogravimetric analysis

To study the stability of the framework of **1**, thermogravimetric analysis (TGA) study was carried out. The TG curve of **1** displays some sharp weight loss from 40 to 210 ℃ corresponding to the loss of the lattice solvent molecules and the evacuation of the coordinated water molecules corresponds to the relatively steady weight loss since 94.81 ℃. The whole structure starts to decompose since 259.3 ℃ (Fig.3).

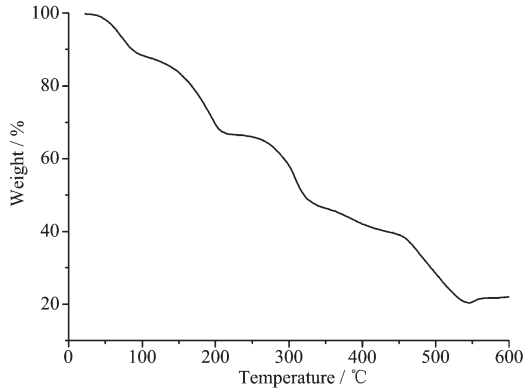

Fig.3　TGA data of sample **1** after washed and soaked with DMF

2.3　Gas adsorption properties

Owing to the microporous structure of **1**, we continued to investigate the gas adsorption/desorption properties of **1**, but unfortunately there are no meaningful N_2 adsorption for **1** and the framework was partially collapsed when guest molecules and coordinated water molecules were evacuated from **1**, which may be attributed to the avulsion of the relatively instable pyrazole-bridged cyclic binuclear by surface tension of solvent molecules as we can see from the sharp changes of PXRD data (Fig.4). Nevertheless, as we measured, **1** can still adsorb a certain amount of CO_2 (24.6 $cm^3 \cdot g^{-1}$ at 273 K, 15.7

$cm^3 \cdot g^{-1}$ at 298 K) (Fig.5) as the UMCs (unsaturated metal sites) and acylamide groups may stay intact in the partially blocked frameworks.

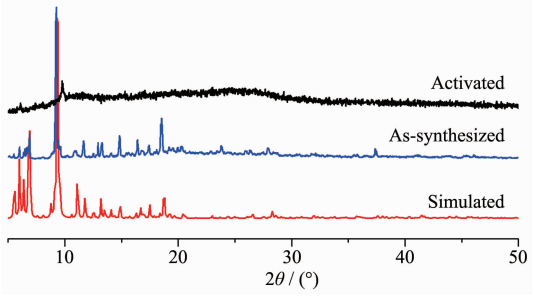

Fig.4 PXRD patterns of **1**

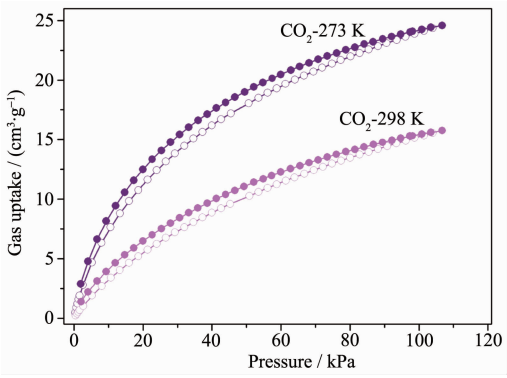

Fig.5 Carbon dioxide adsorption isotherms of **1** at 273 K, 298 K (open ones: adsorption; filled shapes: desorption)

2.4 Iodine sorption

As we deduced, **1** is of great potential in iodine adsorption due to the specific groups in the channels and nearly all the adsorption or exchange process of molecules will proceed in the liquid phase, thus the destructive vacuum environment can be avoided. Therfore, we explored its iodine absorption property. After washed and soaked with DMF for days, airing samples of **1** (40 mg) were immersed in a hexane (3 mL) solution of I_2 (0.01 $mol \cdot L^{-1}$), and then the colour of the crystals deepened from light blue to deep green and finally dark (Fig.6). On the contrary, the dark brown solution of I_2 faded quickly to pale pink in hours (Fig.7a). Confirmed by the PXRD data, high amount of iodine in **1** has nearly no impact on the sensitivity of X-ray of **1** (Fig.8). Although frequentative attempts to get feasible single crystal X-ray diffraction data of I_2@**1** were all unsuccessful which may be due to the reduced crystal quality of **1** after I_2 adsorption, calculated from the thermogravimetric analysis (Fig.9), 1 g of **1** can adsorb nearly 0.49 g of I_2 (2.6 I_2 molecules each formula unit) to get 2.6I_2@**1** and the adsorption amount of I_2 (~ 32.9%) is nearly the sixth highest compared with

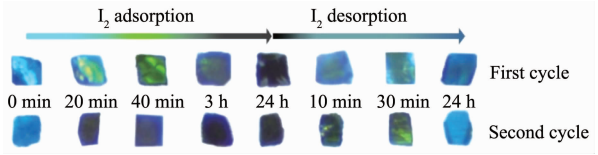

Fig.6 Photographs for **1** of adsorption (hexane) and releasing I_2 (ethanol) in two cycles

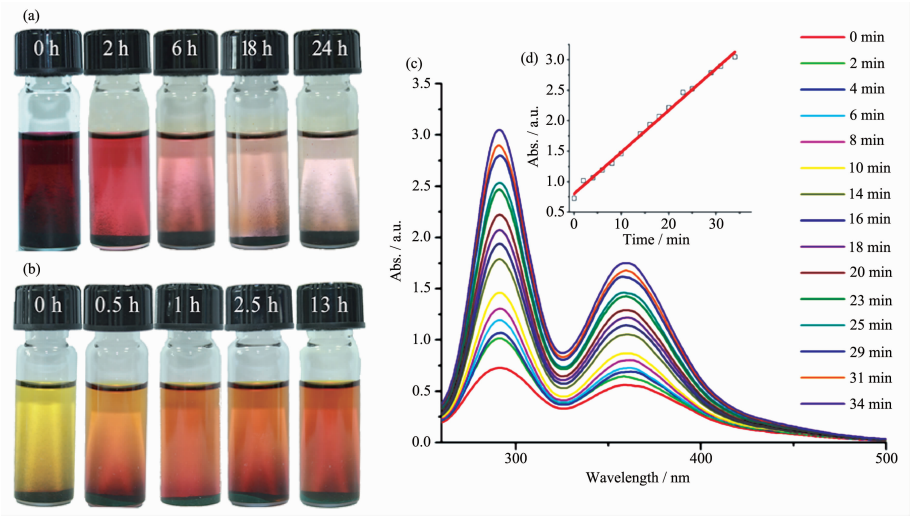

Fig.7 Photographs showing the colour change when **1** (40 mg) was soaked in hexane solution of I_2 (3 mL, 0.01 $mol \cdot L^{-1}$); (b) I_2 release process when I_2@**1** (50 mg) was immersed in EtOH (3 mL); (c) UV-Vis spectra of I_2@**1** for the releasing process of iodine; (d) Linear increase of the absorbance of I_2 in ethanol with time at the beginning

some previously reported MOFs [11]. As a result, an obvious decrease of the fluorescence emission intensity (λ_{ex}=307 nm and λ_{em}=423, 440, 457, 483 nm) emerged upon the entry of I_2 into the host framework of **1** which may be attributed to the host-guest π-bonding and hydrogen-bonding photoinduced electron transfer effect [11-12] (Fig.10) and also indicates that **1** can quickly adsorb iodine molecules.

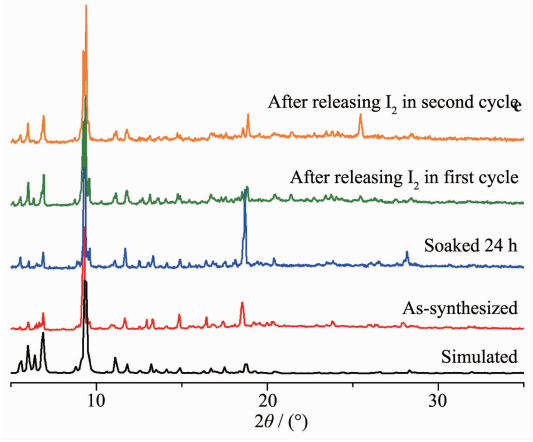

Fig.8　X-ray powder diffraction patterns of **1** after releasing I_2 in first and second cycle, **1** soaked in a hexane solution (0.01 mol·L^{-1}) of I_2 at room temperature for 24 hours, as-synthesized **1** and simulated **1**

Notably, the I_2 desorption of 2.6I_2@**1** seemed more efficiently and **1** is of reversible I_2 adsorption ability. When the crystals of 2.6I_2@**1** were soaked in dry ethanol (3 mL), the colour of the crystals changed gradually from dark to light blue and the colour of the ethanol solution deepened quickly from colourless to

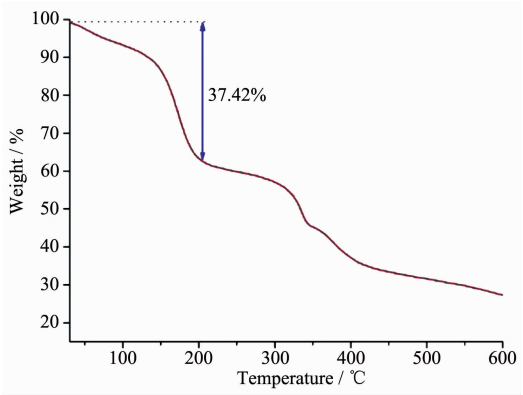

Curve displays some sharp weight loss (~37.42%) from 40 to 210 ℃ corresponding to the loss of the lattice I_2 molecules and the evacuation of the coordinated water molecules

Fig.9　TGA data of 2.6I_2@**1**

dark yellow and stayed the same after one hour′s immersion (Fig.6b). At the same time, the intensity of the fluorescence emission gradually recovered and the structure of **1** stayed intact upon guest exchange just as expected (Fig.8). To further investigate the kinetics of I_2 delivery of 2.6I_2@**1**, the UV-Vis spectra were recorded at room temperature. The absorbance of I_2 in ethanol increases linearly with time at the beginning and the releasing rate becomes slower later as the concentration of I_2 in ethanol increases with time (Fig. 7c,d). To verify the repeatability, the reversible I_2 adsorption process was tested for another cycle and the photographs and PXRD patterns of **1** demonstrated that the I_2 sorption process of **1** is repeatable (Fig.6, 8). As we can see from the above description, there is a great advantage of **1** in reversible iodine adsorption

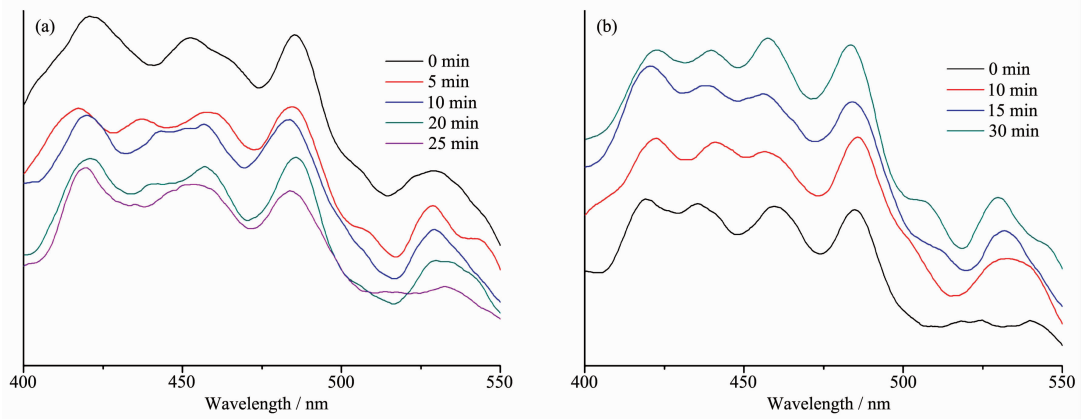

Fig.10　Photoinduced solid state emission spectra of **1** (a) its I_2-loaded samples luminescence change during 0~25 min (λ_{ex}=346 nm and λ_{em}=405 nm); (b) After immersed in ethanol for 30 min, the luminescence intensity of **1** was gradually recovered

which may be attributed to the specific physical environment of the pores, surfaces in **1**. The regular confined micro-pores, abundant regular π-electron walls made of aromatic benzene, pyrazole rings, and the acylamide groups paved levelly along the channel may accumulate the superiority of **1** in iodine adsorption performance as the host-guest π-bonding and hydrogen -bonding effect stabilizes I_2 molecules through $\pi\cdots$I and N–H$\cdots$I interactions[6-7].

3 Conclusions

In summary, by introducing acylamide and aromatic groups, a novel porous Cu-MOF (**1**) has been successfully synthesized based on acylamide tetracid of pyrazole (5,5′-((1*H*-pyrazole-3,5-dicarbonyl)bis (azanediyl))diisophthalic) linker and copper(Ⅱ) salts. In the structure of **1**, there exists microporous square channels surrounded with aromatic benzene and pyrazole rings as well as acylamide groups. Though the structure of **1** is not stable enough in gas adsorption measurement, **1** is still of outstanding performance in reversible adsorption of iodine which may be owing to the hydrogen and π bond donors spreading throughout the channels which may enhance the host-guest interactions between the framework and iodine molecules. Our work presents a conception that the instability of some MOFs after evacuation in gas adsorption may be not be so fatal in the adsorption of other species in the liquid phase, and new strategies and criteria could be adopted when we design and evaluate these MOFs.

Acknowledgements: This work was supported by the National Natural Science Foundation of China (Grant No. 21371150 and 21371091).

References:

[1] (a)Yaghi O M, O′Keeffe M, Ockwig N W, et al. *Nature*, **2003**, **423**:705-714
(b)Sumida K, Rogow D L, Mason J A, et al. *Chem. Rev*., **2012**,**112**:724-781
(c)Kreno L E, Leong K, Farha O K, et al. *Chem. Rev*., **2012**,**112**:1105-1125
(d)Tanabe, Kristine K, Allen C A, et al. *Angew. Chem., Int. Ed.*, **2010**,**49**:9730-9733
[2] (a)Rosenfeld L. *J. Chem. Educ*., **2000**,**77**:984-987
(b)Curtouis B. *Ann. Chim.*, **1813**,**88**:304-310
[3] Lunde. *Chem. Rev*., **1929**,**6**:45-61
[4] Carpenter L J. *Chem. Rev.*, **2003**,**103**:4953-4962
[5] Kyotani M, Matsushita S, Nagai T, et al. *J. Am. Chem. Soc.*, **2008**,**130**:10880-10881
[6] Safarifard V, Morsali A. *CrystEngComm*, **2014**,**16**:8660-8663
[7] Liu Q K, Ma J P, Dong Y B. *Chem. Commun.*, **2011**,**47**:7185 -7187
[8] (a)Sheldrick G M. *SHELXS*-97, *Program for the Solution of Crystal Structures*, University of Göttingen, Germany, **1997**.
(b)Sheldrick G M. *SHELXL*-97, *Program for the Refinement of Crystal Structures*, University of Göttingen, Germany, **1997**.
[9] Spek A L. *J. Appl. Crystallogr.*, **2003**,**36**:7-13
[10]Blatov V A, Peskov M V. *Acta Crystallogr. Sect. B*: *Struct. Sci.*, **2006**,**62**:457-466
[11]He W W, Li S L, Yang G S, et al. *Chem. Commun.*, **2012**, **48**:10001-10003
[12]Zhao B, Chen X Y, Cheng P, et al. *J. Am. Chem. Soc.*, **2004**,**126**:15394-15395